

## Article

# Impact- and Thermal-Resistant Epoxy Resin Toughened with Acacia Honey

Ivana Stajcic <sup>1,\*</sup>, Filip Veljkovic <sup>1</sup>, Milos Petrovic <sup>2</sup>, Suzana Veličkovica <sup>1</sup>, Vesna Radojevic <sup>2</sup>,  
Branislav Vlahović <sup>3</sup> and Aleksandar Stajcic <sup>4</sup>

<sup>1</sup> Department of Physical Chemistry, “Vinča” Institute of Nuclear Sciences—National Institute of the Republic of Serbia, University of Belgrade, Mike Petrovića Alasa 12-14, P.O. Box 522, 11001 Belgrade, Serbia; filipveljkovic@vin.bg.ac.rs (F.V.); vsuzana@vin.bg.ac.rs (S.V.)

<sup>2</sup> Faculty of Technology and Metallurgy, University of Belgrade, 11000 Belgrade, Serbia; mpetrovic@tmf.bg.ac.rs (M.P.); vesnar@tmf.bg.ac.rs (V.R.)

<sup>3</sup> Mathematics and Physics Department, North Carolina Central University, Durham, NC 27707, USA; vlahovic@ncsu.edu

<sup>4</sup> Center for Microelectronic Technologies, Institute of Chemistry, Technology and Metallurgy—National Institute of the Republic of Serbia, University of Belgrade, 11000 Belgrade, Serbia; stajcic@nanosys.ihtm.bg.ac.rs

\* Correspondence: ivana\_r@vinca.rs

**Abstract:** High performance polymers with bio-based modifiers are promising materials in terms of applications and environmental impact. In this work, raw acacia honey was used as a bio-modifier for epoxy resin, as a rich source of functional groups. The addition of honey resulted in the formation of highly stable structures that were observed in scanning electron microscopy images as separate phases at the fracture surface, which were involved in the toughening of the resin. Structural changes were investigated, revealing the formation of a new aldehyde carbonyl group. Thermal analysis confirmed the formation of products that were stable up to 600 °C, with a glass transition temperature of 228 °C. An energy-controlled impact test was performed to compare the absorbed impact energy of bio-modified epoxy containing different amounts of honey with unmodified epoxy resin. The results showed that bio-modified epoxy resin with 3 wt% of acacia honey could withstand several impacts with full recovery, while unmodified epoxy resin broke at first impact. The absorbed energy at first impact was 2.5 times higher for bio-modified epoxy resin than it was for unmodified epoxy resin. In this manner, by using simple preparation and a raw material that is abundant in nature, a novel epoxy with high thermal and impact resistance was obtained, opening a path for further research in this field.

**Keywords:** bio-modifier; acacia honey; epoxy resin; thermal stability; impact-resistant



**Citation:** Stajcic, I.; Veljkovic, F.; Petrovic, M.; Veličkovica, S.; Radojevic, V.; Vlahović, B.; Stajcic, A. Impact- and Thermal-Resistant Epoxy Resin Toughened with Acacia Honey. *Polymers* **2023**, *15*, 2261. <https://doi.org/10.3390/polym15102261>

Academic Editors: Yun Lu, He Liu and Jingpeng Li

Received: 7 April 2023

Revised: 26 April 2023

Accepted: 29 April 2023

Published: 10 May 2023



**Copyright:** © 2023 by the authors. Licensee MDPI, Basel, Switzerland. This article is an open access article distributed under the terms and conditions of the Creative Commons Attribution (CC BY) license (<https://creativecommons.org/licenses/by/4.0/>).

## 1. Introduction

Epoxy resins are widely used materials, due to their suitable properties such as a high Young’s modulus, chemical and thermal resistance, good corrosion resistance, and excellent insulation [1–6]. They were extensively studied for various industrial applications, including construction, automobile manufacture, and military and aerospace industry applications, which require high-performance materials [7–9]. In order to satisfy the application demands, numerous epoxy matrix composite materials with a versatility of ceramic and organic nanoparticles and fiber reinforcements were developed over the years [10,11]. However, cross-linked epoxy shows low toughness, which raises the concern of the composites’ performance under impact. The formation of micro-cracks that are not visible to the naked eye leads to a sudden breakage, which poses a great problem for manufacturers of parts that are placed in critical mechanical points. The heterogeneous nature of microscale epoxy-based composites could also be regarded as a weakness. Fiber-reinforced composites show high impact resistance in the direction of fiber orientation,

while in other directions, damage occurs at low impact. As crack initiation and propagation take place in various ways, such as epoxy cracking, fiber failure, or debonding, it is very difficult to build a prediction model for fracture behavior and the potential absorbed energy [12]. The common challenges with conventional reinforcements include deformation and oxidation of polymer-based fibers, depending on the working conditions. Moisture acts as a plasticizer in epoxy resin, which leads to lowering the glass transition temperature value ( $T_g$ ) and reducing thermal and mechanical performance. Moisture can also induce corrosion in fiberglass, a frequently used reinforcement.

Recently, much attention was given to chemical modifications of epoxy in order to increase its thermal and mechanical properties. Meanwhile, growing environmental concerns, along with finite petrochemical resources, led to a focus on the development of composite materials with reinforcements from renewable resources [13]. In order for such materials to reach their full potential for application, a balance between mechanical performance and environmentally friendly behavior must be achieved. Flax or bamboo fibers, as well as bio-based silica, were proposed as green reinforcements to improve epoxy's mechanical properties [14–16]. It was proven that the effect of various modifying additives and fillers (of natural origin) on the physicochemical and mechanical properties of epoxy polymer composites is determined by many factors. Bekeshev et al. modified diorite with phenyl-terminated agents in order to improve filler/polymer interface interaction, which resulted in increased thermal resistance and mechanical strength [17]. Oladele et al. incorporated eggshell and sisal fibers in an epoxy matrix, improving tensile and flexural strength [18]. The addition of bael shell biochar, proposed by Minugu et al., significantly increased the tensile strength and thermal stability of epoxy [19]. Bezerra et al. recently discovered that the high-load (30 wt%) addition of arapaima fish scales caused structural and mechanical changes in epoxy, resulting in increased hardness [20].

Lignin is one of the main plant constituents, with a high content of functional groups that make it suitable for use as a raw material in the synthesis of bio-based epoxy, as a replacement for the diglycidyl ether of bisphenol A (DGEBA) [21]. However, lignin shows low reactivity, resulting in solid products with low solubility [22]. Lu et al. functionalized epoxy in order to obtain a liquid, which is a more compatible epoxidized compound for the use as a bio-based epoxy. Recently, Xu et al. used gallic and modified tannic acid to synthesize bio-based epoxy resin with increased toughness [23]. Hollande et al. synthesized renewable epoxy bisphenols from ferulic acid and fatty acids [24]. They showed that thermal properties and degradability could be controlled by the different structure and content of the constituents. Although these resins have great potential, the glass transition temperature ( $T_g$ ) is very low, reducing the temperature range for application. Yu et al. prepared bio-based dimer acid diglycidyl ester for the toughening of DGEBA-based epoxy resin [25]. With a small percentage of the toughener, the impact strength was increased by more than two times. However, the  $T_g$  decreased, compared to the  $T_g$  with the unmodified epoxy. A similar trend was observed in soybean oil and saturated-fatty-acids-based modifiers prepared by Hu et al., except that the overall  $T_g$  values were significantly higher when compared to those in a previous study [26]. In order to achieve high-impact strength and compatibility DGEBA-based epoxy resin, Zhang et al. synthesized xylitol-based hyperbranched epoxy toughener, increasing the impact strength by over 200% [27]. With the same aim, Yadav et al. developed bio-rubber from soybean oil, increasing the critical strain energy by 500% [28]. Furthermore, Mi et al. modified konjac fly powder and achieved an increase in impact strength of over 100% with 20% of the toughener in DGEBA [29]. They attributed the improved impact behavior to the free-volume increase that resulted in internal stress reduction. Based on these studies, it can be seen that bio-based modifications of epoxy represent a great challenge with great potential for application and for the development of green technologies.

Honey is known for heterogeneous structure, with reactive components that could be used in materials chemistry. Along with carbohydrates such as fructose and glucose, many

other substances can be found in honey, depending on the plant source and geographical origin [30].

Along with that, honey is a low cost, low moisture containing and abundant in nature raw material [31]. In the light of these facts, acacia honey was used in this research as a modifier for DGEBA based epoxy, with the aim of improving poor impact resistance. Acacia honey was chosen as a monofloral honey, common in Serbia. It was added in DGEBA/DETA system during the cross-linking at room temperature, and the resulting material was investigated from the thermal, mechanical, and structural aspect. After preparing samples with 1, 3, and 6 wt%, epoxy modified with 3 wt% of honey was chosen for further investigations that revealed high thermal and mechanical performance, opening the path for further research in this direction.

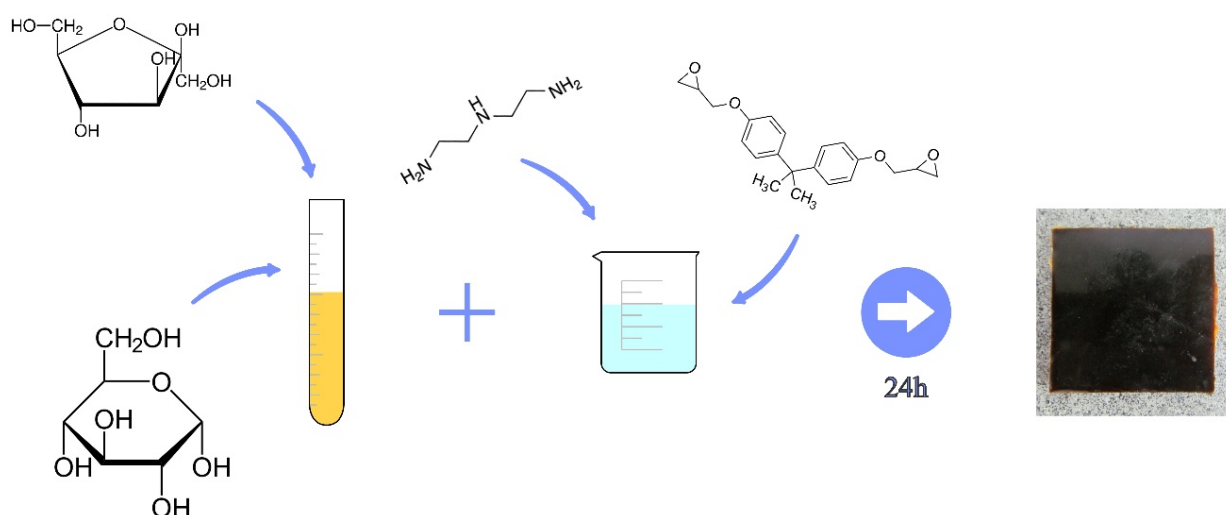
## 2. Materials and Methods

### 2.1. Materials

Diglycidyl ether of bisphenol A (DGEBA)-based epoxy resin and diethylenetriamine (DETA)-based hardener were purchased from R&G Faserverbundwerkstoffe GmbH, Composite Technology, Waldenbuch, Germany. Acacia honey, manufactured by 'Mepolis', Belgrade, Serbia (glucose + fructose: >70%, water: <20%, sucrose < 5%, 1.36 g/cm<sup>3</sup>) was used as the epoxy modifying agent.

### 2.2. Preparation of Samples

First, DGEBA and DETA were mixed in 20:9 volume ratios, in accordance with manufacturer's instructions. After 2 minutes of vigorous mixing, 1, 3, or 6 wt% of acacia honey was added, and the mixing was continued for another 2 minutes. The mixture was poured into a silicone mold and left for 24 h at 25 °C to cross-link and solidify. Compared to the unmodified epoxy, gel time was reduced from 40 to 15 minutes. The samples were prepared for a controlled energy impact test with dimensions 60 mm × 60 mm × 6 mm. Scheme 1 illustrates the preparation of modified epoxy. Unmodified epoxy was labeled as E; epoxy modified with acacia honey was labeled in accordance with honey concentration: EH1 for 1 wt%, EH3 for 3 wt%, and EH6 for 6 wt% of honey.



**Scheme 1.** Preparation of bio-modified epoxy.

### 2.3. Characterization of E and EH

Morphological differences between E and EH were recorded with a Field Emission Scanning Electron Microscope—FESEM (TESCAN MIRA 3, Brno, Czech Republic), surfaces were sputtered with gold. Structural changes with the addition of honey to epoxy resin were investigated using Fourier transform infrared—FTIR (Hartmann & Braun, MB-series, Bockenheim, Germany), 4000 and 400 cm<sup>-1</sup>, resolution of 4 cm<sup>-1</sup>. The thermal stability

of EH was monitored using a Simultaneous Thermal Analyzer (STA) (TGA-DTG-DTA) (Netzsch STA 449 Jupiter F5, Bayern, Germany), in the temperature range from room temperature to 600 °C, with a heat rate of 10 °C/min. The sample mass was  $10 \pm 0.5$  mg. The measurements were performed in synthetic air (21 vol% O<sub>2</sub> + 79 vol% N<sub>2</sub>).

The difference in impact resistance of E, EH1, EH3, and EH6 was investigated with the High Speed Puncture Impact Testing Machine (HYDROSHOT HITS-P10, Shimadzu, Kyoto, Japan). Absorbed energy (total absorbed energy- $E_{tot}$  and energy at maximum load- $E_{fmax}$ ) values were calculated automatically from the load-time diagram. The diameter of the striker was 12.7 mm, with a hemispherical head; the set impact force was 10 kN. For samples E and EH1, impact velocity and depth were 0.05 m/s and 1 mm, respectively. A variation of impact depth and velocity (Table 1) was performed for samples EH3 and EH6, in order to investigate impact resistance.

**Table 1.** Impact test parameters.

Sample	EH3		EH6	
	Impact Velocity, m/s	Impact Depth, mm	Impact Velocity, m/s	Impact Depth, mm
1	0.05	1	0.05	1
2	0.1	2	1	6
3	0.2	2	-	-
4	0.2	3	-	-
5	0.3	3	-	-
6	0.5	3	-	-
7	0.5	6	-	-
8	1.0	6	-	-

### 3. Results and Discussion

#### 3.1. FESEM Analysis

The toughening effect of honey addition to epoxy could be analyzed through the crack propagation pattern observed on FESEM images (Figures 1 and 2). Depending on the crack path, there are different toughening mechanisms. In our case, the fracture surface of E shows typical brittle failure with polymer plastic deformation causing river-like path lines (Figure 1). This type of crack spreading is correlated with low fracture toughness [32].

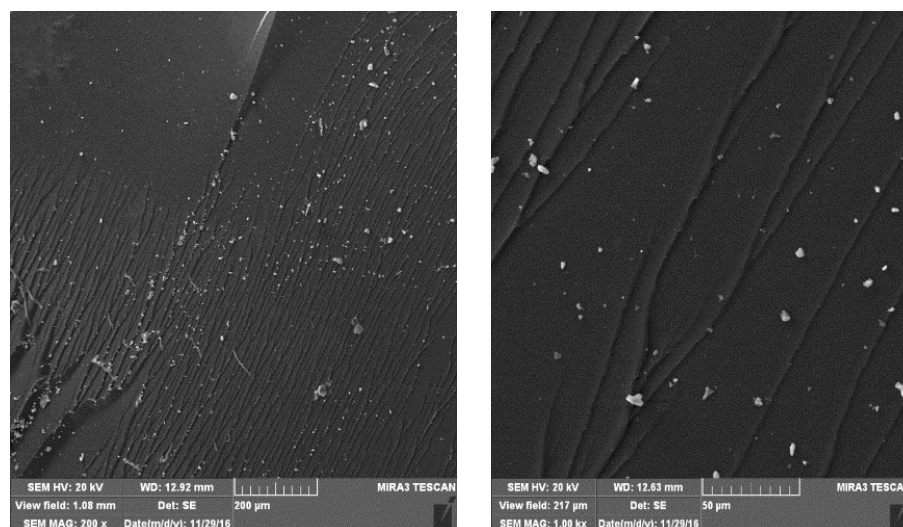


**Figure 1.** Fracture surface of E.

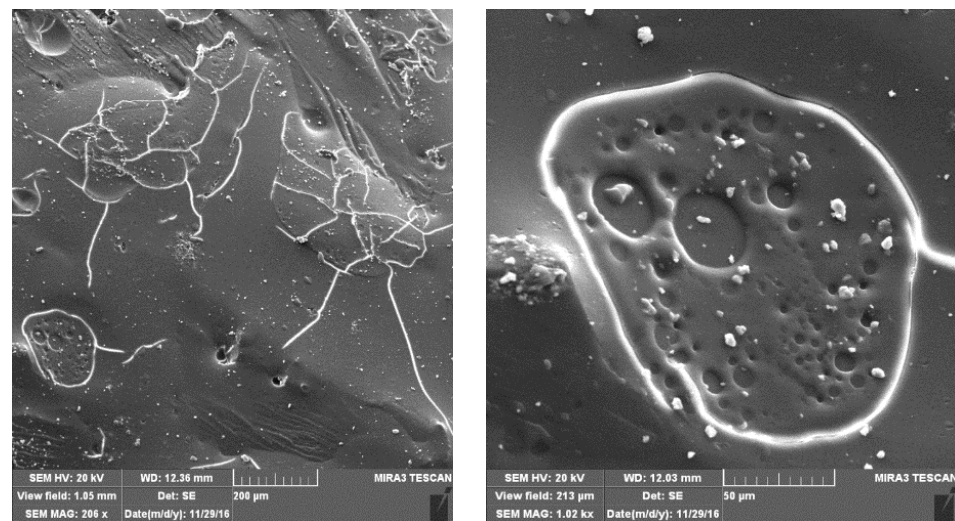


**Figure 2.** Fracture surface of EH3.

On the other side, the fracture surface of EH3 showed higher roughness, which was directly connected to an increased toughness in the material. The surface was covered with cracks with a changeable path, with separate phases acting as tougheners. Obviously, crack arrest occurred around the phase-separated microstructural formations. The secondary phase was not separated from the rest of the surface during impact, indicating high compatibility between epoxy and the modified moiety. The dominant toughening mechanism was crack-branching that caused local energy dissipation and the formation of secondary cracks. In this manner, epoxy modified with acacia honey showed a crack propagation pattern similar to the nanocomposites with incorporated rigid nanoparticles [33,34]. In addition, the strong plastic deformation of EH3 also indicated higher toughness compared to E.

On the part of the upper surface of EH3, pores filled with phase-separated spheres were found, presumably of the partly unreacted honey, which formed microcapsules (Figure 3).

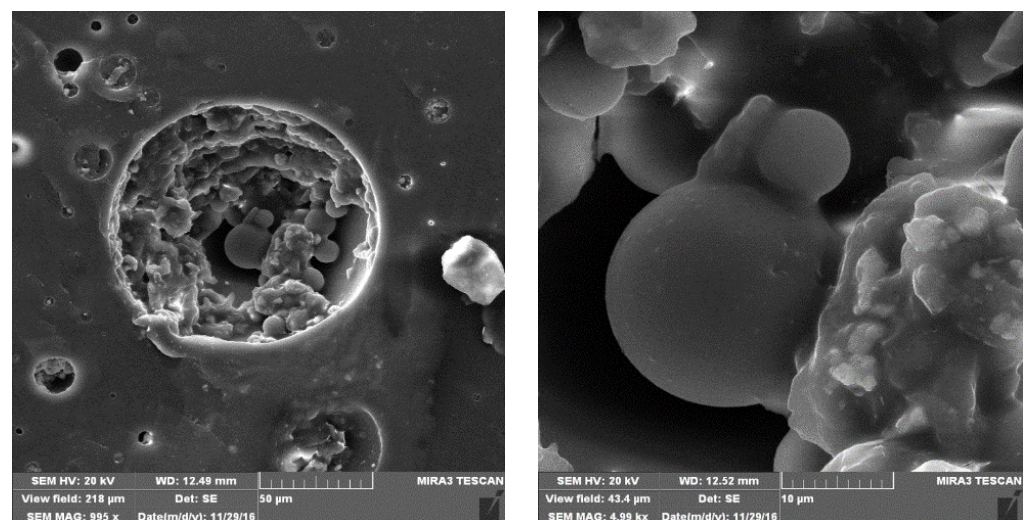


**Figure 3.** FESEM images of microcapsules at the surface of EH3.

Sample EH6 (Figure S1) showed the presence of large pores filled with partly unreacted honey throughout the entire volume, which was expected to result in lower mechanical performance compared to EH3.

### 3.2. FTIR Analysis

Honey is mostly composed of water and simple sugars, such as fructose and glucose, although it contains proteins, vitamins, minerals, and many other substances in small amounts [31,35]. The heterogeneity of acacia honey structure enabled different sets of complex chemical reactions when it reached contact with a suitable medium. In our case, we presumed that after DGEBA-based epoxide was mixed with DETA based cross-linker, the exothermic reaction of cross-linking was enough to initiate Maillard reaction of glucose and fructose in honey with  $\text{-NH}_2$ , resulting in the formation of aldol condensation products [36]. Scheme 1 shows the sample of modified epoxy, where the brown coloration characteristic of Maillard reaction products can be observed [37]. In order to establish structural changes in epoxy after the addition of honey (H), FTIR spectroscopy was performed (Figure 4). The spectrum range ( $4000$  to  $400\text{ cm}^{-1}$ ) was divided into two regions to highlight structural differences between E and EH.

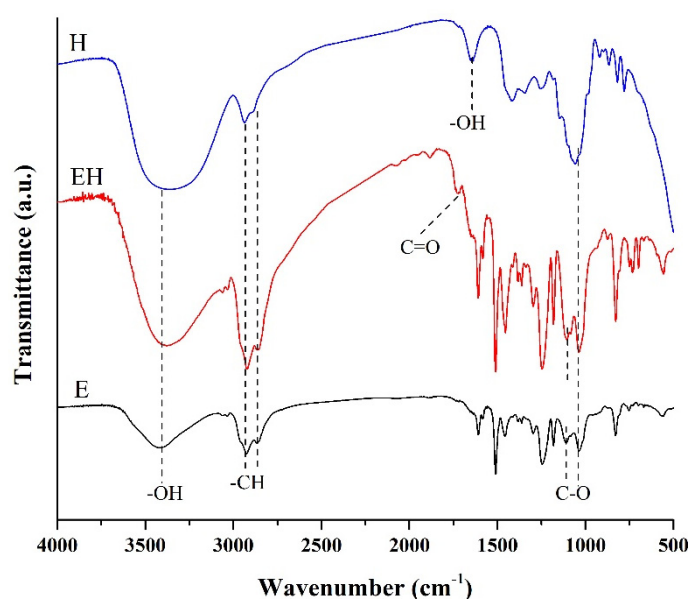


**Figure 4.** FTIR spectra of pure epoxy, honey, and bio-modified epoxy.

#### 3.2.1. The Region $4000\text{--}1300\text{ cm}^{-1}$

All spectra have broad bands from the H bonded  $\text{-OH}$  group in the region from  $3350$  to  $3400\text{ cm}^{-1}$ . However, in the spectrum of AH, this band was broader, indicating a higher concentration of hydroxyl groups that may originate from present moisture and carbohydrates. Aromatic  $\text{-CH}$  stretch was present in E and EH at  $3063\text{ cm}^{-1}$  and  $3032\text{ cm}^{-1}$ , coming from phenolic groups in epoxy. Asymmetric  $\text{-CH}$  stretching can be seen in all the spectra around  $2935\text{ cm}^{-1}$ , as well as symmetric at  $2870\text{ cm}^{-1}$ .

E and EH3 showed small, broad bands around  $1950\text{ cm}^{-1}$  and  $1884\text{ cm}^{-1}$ , originating from double-bonded carbon atoms. The most interesting structural change was observed by the appearance of a peak at  $1721\text{ cm}^{-1}$ , which comes from carbonyl groups that formed after the reaction of H and E. This peak was assumed to be from aldehyde  $\text{C=O}$ , which formed after the reaction of reducing sugars with amine [38]. In the spectrum of H at  $1646\text{ cm}^{-1}$ , a peak appeared that is related to the presence of moisture in H, which could overlap with  $1^\circ$  amide  $\text{C=O}$ , presumably from the proteins [39,40].

#### 3.2.2. The Region $1300\text{--}400\text{ cm}^{-1}$

In the region from At  $1245\text{ cm}^{-1}$ ,  $1184\text{ cm}^{-1}$ ,  $1107\text{ cm}^{-1}$  and  $1033\text{ cm}^{-1}$ ,  $\text{C-O}$  stretching vibrations were observed in the spectra of E and EH3 [41–43]. The H sample had only two peaks in that range, at  $1252\text{ cm}^{-1}$  and  $1052\text{ cm}^{-1}$ ,  $\text{C-O}$  stretching from  $\text{C-OH}$ , characteristic for fructose and glucose carbohydrates. The absence of a band around  $1185\text{ cm}^{-1}$  proved

that our H sample did not contain sucrose [39]. Out-of-plane  $\nu_{CH}$  bending was observed in all three spectra in the region  $916\text{--}697\text{ cm}^{-1}$  [44–46]. Stronger peaks in EH3 indicate the presence of carbohydrates [47].

### 3.3. Thermogravimetric Analysis (TGA)

In order to investigate the thermal stability of epoxy modified using acacia honey, simultaneous thermal analysis was performed in the air. Following the assumptions made by structural and morphological analyses, structures formed during processing should have resulted in bio-modified epoxy resin with high thermal stability. The curves obtained from TGA-DTG-DTA for the most representative sample, EH3, are presented in Figure 5. The TGA curve of EH3 showed a weight loss of 2.7% in the region around  $35\text{--}165\text{ }^{\circ}\text{C}$ , which indicates a very low presence of water and unreacted compounds with a low boiling point [48]. A small DTG peak was detected at  $133\text{ }^{\circ}\text{C}$  in this region. The degradation of epoxy moiety due to thermal oxidation reactions that involve chain scission was observed in two stages [45]. The first stage was from  $165\text{ }^{\circ}\text{C}$  to  $390\text{ }^{\circ}\text{C}$ , with a strong DTG peak at  $279\text{ }^{\circ}\text{C}$ , which is in accordance with the literature and our previous investigation on epoxy thermal stability [49,50]. Weight loss in this region was 22%, which corresponds to a minor endothermic peak at DTA.

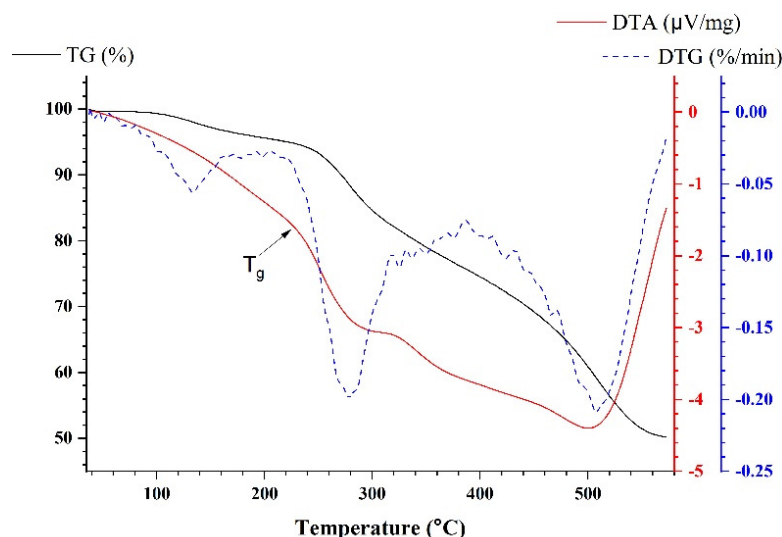


**Figure 5.** TGA-DTG-DTA curves for EH3.

The second degradation stage was from  $390\text{ to }570\text{ }^{\circ}\text{C}$ , where the largest weight loss of 25% occurred, with a strong DTG peak at  $508\text{ }^{\circ}\text{C}$  [51]. In this region, the degradation of epoxy benzene rings occurred [52].

The char yield at  $570\text{ }^{\circ}\text{C}$  was 50%, which was significantly higher compared to the previous research regarding modified epoxies with improved thermal stability [25,53]. This stability could be explained by highly stable condensed structure that evolved during the initial heating of the sample [54,55]. This stability is similar to the reported phenolic condensed structures, which indicates that reactions including the DGEBA moiety resulted in highly stable modified epoxy [56].  $T_5$ ,  $T_{10}$ , and  $T_{30}$  are presented in Table 2.

**Table 2.** Comparison of thermal analysis data for EH3 and E.

	$T_5, ^{\circ}\text{C}$	$T_{10}, ^{\circ}\text{C}$	$T_{30}, ^{\circ}\text{C}$	$T_{\text{hri}}, ^{\circ}\text{C}$	$T_g, ^{\circ}\text{C}$
EH3	221.5	271.1	443.5	173.8	228.0
E	115.3	244.7	290.3	107.9	102.8

The heat resistance index ( $T_{hri}$ ) (Table 2) was calculated according to Equation (1) [52]:

$$T_{hri} = 0.49 \times [T_5 + 0.6 \times (T_{30} - T_5)] \quad (1)$$

This value was comparable to epoxy reinforced with multi-walled carbon nanotubes, which revealed the potential of honey as a modifier. Compared to the highly stable DGEBA epoxy used by Mi et al.,  $T_5$  and  $T_{10}$  of EH3 were lower, but compared to their reported  $T_{max}$  value of 368 °C, EH3  $T_{50}$  of 570 °C was substantially higher [29].

The glass transition temperature ( $T_g$ ) determined by DTA (Table 2) was significantly higher compared to the commercial epoxy, especially since  $T_g$  depends on a curing temperature, which was 25 °C in our case [57–59].

For comparison, values for neat epoxy presented in Table 2 (Supplementary Material, Figure S2) show that  $T_5$ ,  $T_{10}$ , and  $T_{30}$ , and  $T_{hri}$  were much lower than EH3.  $T_{50}$  was 382.7 °C. With the exception of  $T_{50}$ , values were quite low compared to the cured DGEBA resin found in the literature, probably due to less cross-linking achieved without higher-temperature post-curing [29,60]. The same was observed for the neat epoxy  $T_g$  value (Figure S3, Table 2), which was more than 20 °C lower compared to the epoxy used by Yu et al. [25].

### 3.4. Impact Test

The energy absorbed during the impact can be divided in the following phases:

- The first phase represents the energy absorbed through the initial creation of the crack;
- The second phase represents the energy absorbed during the propagation and development of the crack until the failure of the material.

The first phase involves the elastic response of the material and plastic deformation, which is characteristically low for fully cured epoxy resins. The maximum load ( $F_{max}$ ) is reached at the end of this phase. The energy absorbed by material at this moment is denoted as  $E_{fmax}$ . The second phase starts when the crack forms, leading to a significant deterioration of mechanical properties until the breakage or rupture. Total absorbed energy ( $E_{tot}$ ) represents energy absorbed from the beginning of the controlled energy impact test until the load drops below zero, which is considered the end of the test. There are four common types of failure, corresponding to the material's plastic deformation propensity. The first one is brittle failure, typical for ceramic materials and rigid polymer structures, such as cross-linked polymers that form 3D covalently bonded networks. This type of failure is described by no or very small plastic deformation with fast fracture, and low  $E_{tot}$  value. Brittle-ductile fracture is the second type, characterized by a small plastic deformation before breakage. Materials that show ductile-brittle failure (third type) have the ability to plastically deform and absorb more energy during the impact. Extensive plastic deformations are distinctive feature of the fourth type of failure, corresponding to the large  $E_{tot}$  value.

Figure 6 shows photographs of E, EH1, EH3, and EH6 after the first impact, while corresponding load-time curves obtained from the controlled energy impact test can be seen in Figure 7. The surface of EH6 (Figure 6d) was covered with discontinuous pores as a consequence of increased phase separation in bio-modified resin. Unmodified epoxy showed typical ductile failure because full cross-linking could not be achieved without high-temperature post-curing [40]. After the first impact, samples E and EH1 were completely destroyed. On the other hand, it can be seen that EH3 was barely damaged after the first impact, while EH6 was damaged but not completely destroyed. Furthermore, EH3 showed more brittle-ductile failure, which is in accordance with thermal analysis that indicated the existence of a rigid condensed structure, compared to the ductile failure of room-temperature cured E, which showed poor thermal stability. This occurrence lead to performing series of impacts in order to establish the impact resistance potential of EH3.



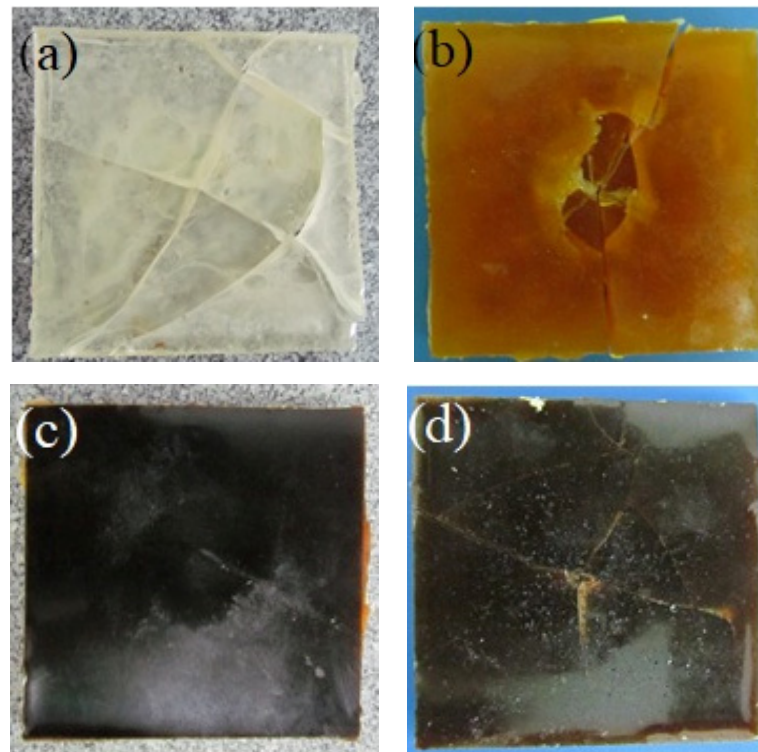


Figure 6. Photographs of: (a) E, (b) EH1, (c) EH3, and (d) EH6 after the first impact.

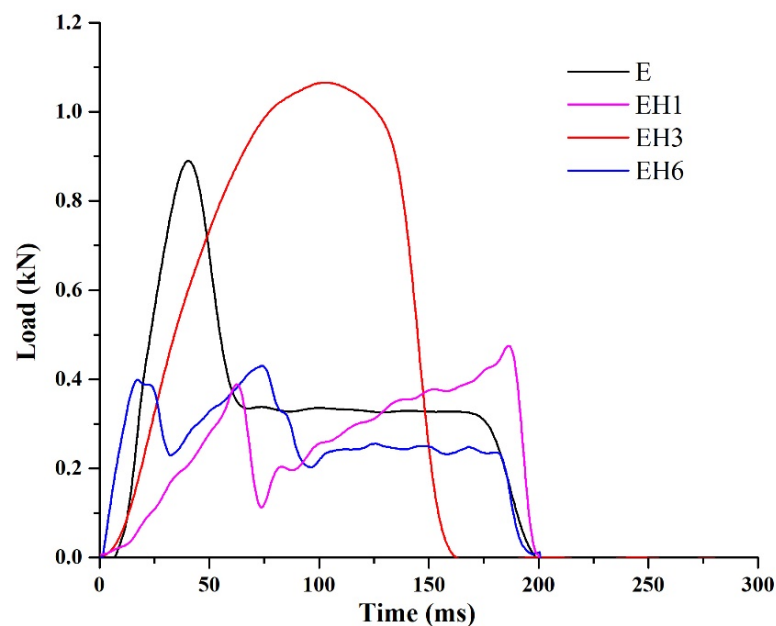
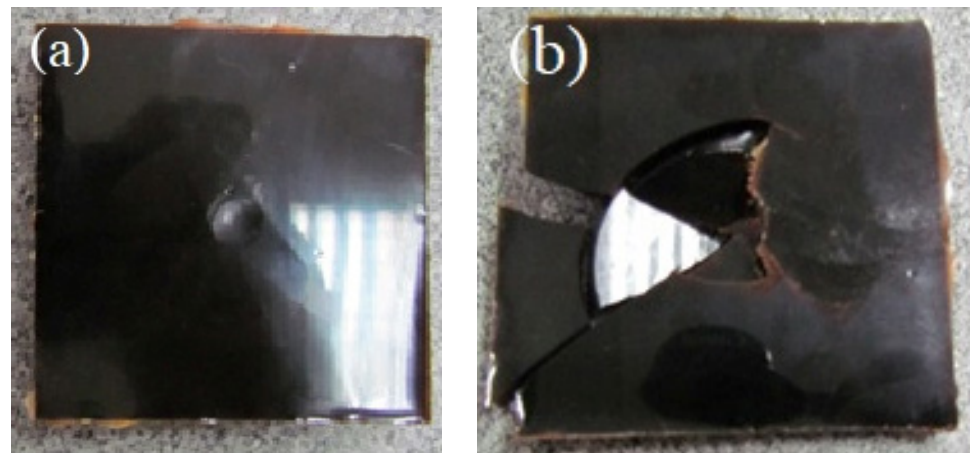


Figure 7. Load-time curves from the first impact by the controlled energy impact test.

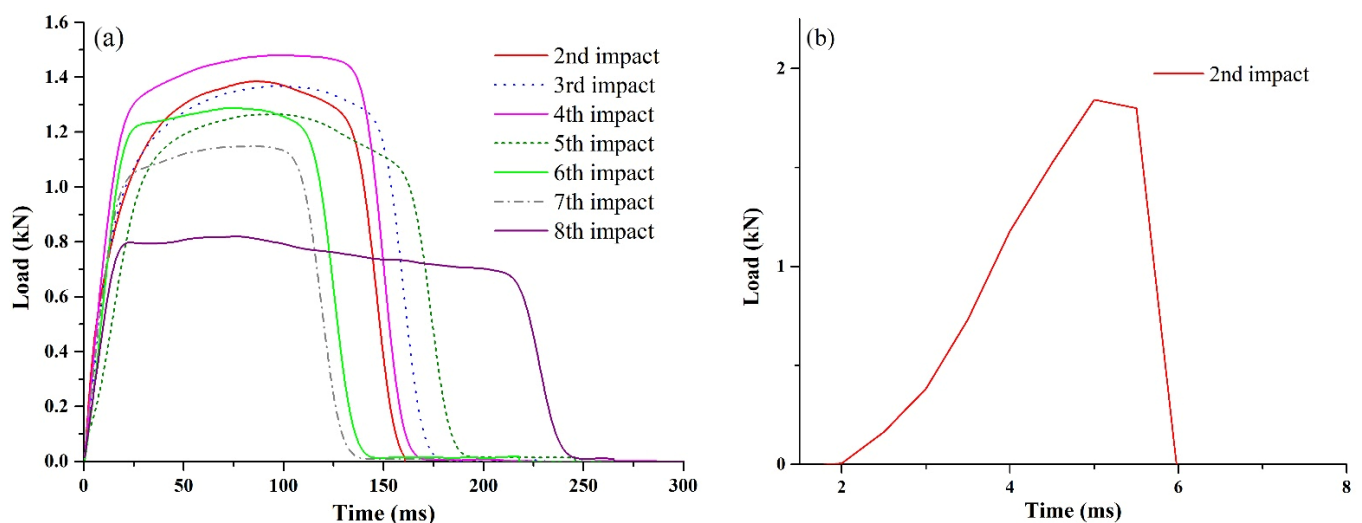
EH3 was punctured eight times with different impact velocities and puncture depths. After the seventh impact, lower absorbed energies were measured as a consequence of the initiated damage from the previous impacts. The sample was left at room temperature for 24 h, after which EH3 returned to its original shape. On the other side, EH6 failed after the second impact, which was consistent with the indications made after the morphological analysis. Figure 8 shows photographs of EH3 after the seventh impact and punctured EH3.



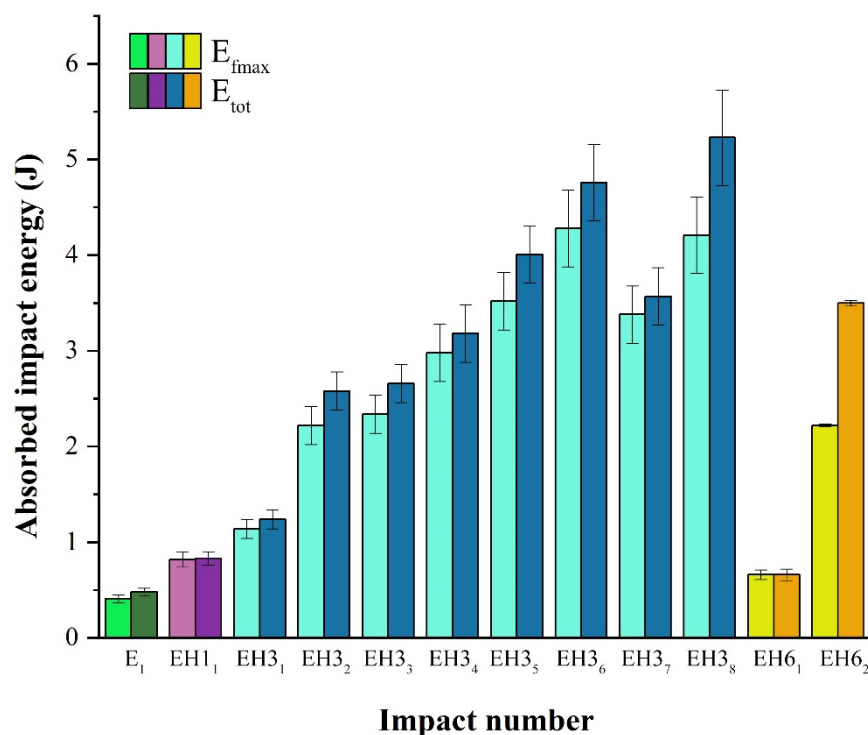
**Figure 8.** Photographs of EH3: (a) after the 7th impact and (b) punctured EH.

Figure 9 represents load-time curves from the second to eighth impact of EH3 (Figure 9a) and the second impact of EH6 (Figure 9b).  $E_{fmax}$  and  $E_{tot}$  for all the samples are presented in Figure 10. During the first impact, E absorbed 0.48 J with the failure of the material, which is consistent with the low toughness of neat epoxy observed on FESEM images [32]. EH1 showed a transition from ductile to brittle failure, with approximately two times higher absorbed energy than E, while EH3 absorbed around 2.5 times more energy with barely visible damage. EH6 showed weaker toughness compared to EH1 and EH3, absorbing 0.66 J. However, unlike EH1, it was not completely broken after the first impact.

On second impact, both  $E_{fmax}$  and  $E_{tot}$  increased in EH3, to 2.22 J and 2.58 J, respectively. The brittle-ductile failure mode remained, in the absence of material failure. The shape of the load-time curve varied from impact to impact, from brittle-ductile to ductile. At the seventh impact, both absorbed energy values decreased compared to the sixth impact, which indicates the beginning of EH3 failure.  $E_{fmax}$  decreased by 20%,  $E_{tot}$  by 25%, but the sample did not break. However, after the sample was left for 24 h at room temperature, impact strength recovery occurred, which was demonstrated by the highest  $E_{fmax}$  and  $E_{tot}$  values observed at the final, eighth impact, where the 1 m/s impact velocity was set and the depth was 6 mm, leading to a puncture of EH3.



**Figure 9.** Load-time curves from controlled energy impact test for (a) EH3 and (b) EH6.



**Figure 10.** Absorbed energy values for E, EH1, EH3, and EH6.

EH6 showed brittle failure during the second impact, as a consequence of the large crack that formed after the first impact. The absorbed energy increased to 3.50 J, but the sample was destroyed, which could be a consequence of an increased phase separation caused by unreacted components. This separation leads to the formation of large pores that could have weakened the sample after the crack initiation (Figure S3). According to the impact test results, 3 wt% is the optimal concentration of honey in epoxy for achieving highly impact-resistant bio-modified resin.

#### 4. Conclusions

This study investigated the potential of honey as a toughener for DGEBA-based epoxy resin. After the addition of different amounts of honey to the DGEBA/DETA system, aldol condensation products formed, which were observed as a separate phase that was responsible for the toughening of the resin. Structural analysis revealed the formation of an aldehyde carbonyl group at  $1721\text{ cm}^{-1}$ , which presumably formed after the reaction of sugars in honey with DETA. Thermal analysis of the sample with 3 wt% of honey showed a high char yield of 50% at  $570\text{ }^\circ\text{C}$ , which is a consequence of DGEBA moiety participation in the reaction with honey, resulting in stable phenolic condensed structures. The heat resistance index was  $173.8\text{ }^\circ\text{C}$ , which is considered very high, as was the glass transition temperature of  $228\text{ }^\circ\text{C}$ . The influence of honey concentration in epoxy on impact resistance was investigated with a controlled energy impact test, and it was established that bio-modified epoxy with 3 wt% withstood several impacts without failure, absorbing the highest amount of energy during the final stroke, leading to the conclusion that it was the optimal amount for obtaining significantly toughened epoxy resin. In light of the presented results, honey proved to be an excellent bio-modifier, which also contributes to the expansion of investigation in the field of bio-based tougheners for polymeric materials.

**Supplementary Materials:** The following supporting information can be downloaded at: <https://www.mdpi.com/article/10.3390/polym15102261/s1>, Figure S1: FESEM image of EH6; Figure S2: TGA curve for neat epoxy in air; Figure S3: DSC curve for neat epoxy in air.

**Author Contributions:** Conceptualization, I.S. and A.S.; methodology, I.S.; validation, I.S., A.S., and V.R.; formal analysis, F.V., S.V., and M.P.; investigation I.S. and V.R.; writing—original draft preparation, I.S. and A.S.; writing—review and editing, V.R. and B.V.; visualization, A.S.; funding acquisition, B.V. All authors have read and agreed to the published version of the manuscript.

**Funding:** This work was financially supported by the North Carolina Central University, USA, NSF DMR EIR 2101041, NSF DMR PREM 2122044, and DOE/NNSA NA0003979 awards and Ministry of Education, Science and Technological Development of the Republic of Serbia (Grant Nos. 451-03-47/2023-01/200017 and 451-03-47/2023-01/200026).

**Institutional Review Board Statement:** Not applicable.

**Data Availability Statement:** The data presented in this study are available on request from the corresponding author. The data are not publicly available due to privacy.

**Conflicts of Interest:** The authors declare no conflict of interest. The funders had no role in the design of the study; in the collection, analyses, or interpretation of data; in the writing of the manuscript; or in the decision to publish the results.

## References

1. Westover, A.S.; Baer, B.; Bello, B.H.; Sun, H.; Oakes, L.; Bellan, L.M.; Pint, C.L. Multifunctional high strength and high energy epoxy composite structural supercapacitors with wet-dry operational stability. *J. Mater. Chem. A* **2015**, *3*, 20097–20102. [[CrossRef](#)]
2. Wan, J.; Gan, B.; Li, C.; Molina-Aldareguia, J.; Kalali, E.N.; Wang, X.; Wang, D.Y. A sustainable, eugenol-derived epoxy resin with high biobased content, modulus, hardness and low flammability: Synthesis, curing kinetics and structure–property relationship. *Chem. Eng. J.* **2016**, *284*, 1080–1093. [[CrossRef](#)]
3. Wang, H.; Liu, Z.; Wang, E.; Zhang, X.; Yuan, R.; Wu, S.; Zhu, Y. Facile preparation of superamphiphobic epoxy resin/modified poly(vinylidene fluoride)/fluorinated ethylene propylene composite coating with corrosion/wear-resistance. *Appl. Surf. Sci.* **2015**, *357*, 229–235. [[CrossRef](#)]
4. Wang, Y.; Yu, J.; Dai, W.; Song, Y.; Wang, D.; Zeng, L.; Jiang, N. Enhanced thermal and electrical properties of epoxy composites reinforced with graphene nanoplatelets. *Polym. Compos.* **2015**, *36*, 556–565. [[CrossRef](#)]
5. Barbosa, A.Q.; da Silva, L.F.M.; Abenojar, J.; Figueiredo, M.; Öchsner, A. Toughness of a brittle epoxy resin reinforced with micro cork particles: Effect of size, amount and surface treatment. *Compos. B Eng.* **2017**, *114*, 299–310. [[CrossRef](#)]
6. Wang, R.; Zhuo, D.; Weng, Z.; Wu, L.; Cheng, X.; Zhou, Y.; Wang, J.; Xuan, B. A novel nanosilica/graphene oxide hybrid and its flame retarding epoxy resin with simultaneously improved mechanical, thermal conductivity, and dielectric properties. *J. Mater. Chem. A* **2015**, *3*, 9826–9836. [[CrossRef](#)]
7. Wang, T.; Song, B.; Wang, L. A new filler for epoxy resin: Study on the properties of graphite carbon nitride (g-c3n4) reinforced epoxy resin composites. *Polymers* **2020**, *12*, 76. [[CrossRef](#)]
8. Ramesh, M. Flax (*Linum usitatissimum* L.) fibre reinforced polymer composite materials: A review on preparation, properties and prospects. *Prog. Mater. Sci.* **2019**, *102*, 109–166. [[CrossRef](#)]
9. Xu, Y.-J.; Chen, L.; Rao, W.-H.; Qi, M.; Guo, D.-M.; Liao, W.; Wang, Y.-Z. Latent curing epoxy system with excellent thermal stability, flame retardance and dielectric property. *Chem. Eng. J.* **2018**, *347*, 223–232. [[CrossRef](#)]
10. Chee, S.S.; Jawaid, M. The Effect of Bi-Functionalized MMT on Morphology, Thermal Stability, Dynamic Mechanical, and Tensile Properties of Epoxy/Organoclay Nanocomposites. *Polymers* **2019**, *11*, 2012. [[CrossRef](#)] [[PubMed](#)]
11. Li, S.; Wu, Q.; Zhu, H.; Lin, Q.; Wang, C. Impact Resistance Enhancement by Adding Core-Shell Particle to Epoxy Resin Modified with Hyperbranched Polymer. *Polymers* **2017**, *9*, 684–695. [[CrossRef](#)] [[PubMed](#)]
12. Skorb, E.V.; Andreeva, D.V. Self-healing properties of layer-by-layer assembled multilayers. *Polym Int.* **2015**, *64*, 713–723. [[CrossRef](#)]
13. Vinod, A.; Sanjay, M.R.; Suchart, S.; Jyotishkumar, P. Renewable and sustainable biobased materials: An assessment on biofibers, biofilms, biopolymers and biocomposites. *J. Clean. Prod.* **2020**, *258*, 120978. [[CrossRef](#)]
14. Al-Hajaj, Z.; Zdero, R.; Bougherara, H. Mechanical, morphological, and water absorption properties of a new hybrid composite material made from 4 harness satin woven carbon fibres and flax fibres in an epoxy matrix. *Compos. A Appl. Sci. Manuf.* **2018**, *115*, 46–56. [[CrossRef](#)]
15. Chee, S.S.; Jawaid, M.; Sultan, M.T.H.; Allothman, O.Y.; Abdullah, L.C. Thermomechanical and dynamic mechanical properties of bamboo/woven kenaf mat reinforced epoxy hybrid composites. *Compos. B Eng.* **2019**, *163*, 165–174. [[CrossRef](#)]
16. Alshahrani, H.; Arun Prakash, V.R. Thermal, mechanical and barrier properties of rice husk ash biosilica toughened epoxy biocomposite coating for structural application. *Prog. Org. Coat.* **2022**, *172*, 107080. [[CrossRef](#)]
17. Bekeshev, A.; Mostovoy, A.; Kadykova, Y.; Akhmetova, M.; Tastanova, L.; Lopukhova, M. Development and Analysis of the Physicochemical and Mechanical Properties of Diorite-Reinforced Epoxy Composites. *Polymers* **2021**, *13*, 2421. [[CrossRef](#)]
18. Oladele, I.O.; Makinde-Isola, B.A.; Adediran, A.A.; Oladejo, M.O.; Owa, A.F.; Olayanju, T.M.A. Mechanical and wear behaviour of pulverised poultry eggshell/sisal fiber hybrid reinforced epoxy composites. *Mater. Res. Express* **2020**, *7*, 045304. [[CrossRef](#)]

19. Minugu, O.P.; Gujjala, R.; Shakuntala, O.; Manoj, P.; Chowdary, M.S. Effect of biomass derived biochar materials on mechanical properties of biochar epoxy composites. *Proc. IMechE Part C J. Mech. Eng. Sci.* **2021**, *235*, 5626–5638. [[CrossRef](#)]
20. Bezerra, W.B.A.; Monteiro, S.N.; Oliveira, M.S.; da Luz, F.S.; da Costa Garcia Filho, F.; da Cruz Demosthenes, L.C.; Costa, U.O. Processing and characterization of Arapaima gigas scales and their reinforced epoxy composites. *J. Mater. Res. Technol.* **2020**, *9*, 3005–3012. [[CrossRef](#)]
21. Asada, C.; Basnet, S.; Otsuka, M.; Sasaki, C.; Nakamura, Y. Epoxy resin synthesis using low molecular weight lignin separated from various lignocellulosic materials. *Int. J. Biol. Macromol.* **2015**, *74*, 413–419. [[CrossRef](#)] [[PubMed](#)]
22. Lu, X.; Gu, X. Fabrication of a bi-hydroxyl-bi-DOPO compound with excellent quenching and charring capacities for lignin-based epoxy resin. *Int. J. Biol. Macromol.* **2022**, *205*, 539–552. [[CrossRef](#)] [[PubMed](#)]
23. Xu, J.; Liu, X.; Fu, S. Bio-based epoxy resin from gallic acid and its thermosets toughened with renewable tannic acid derivatives. *J. Mater. Sci.* **2022**, *57*, 9493–9507. [[CrossRef](#)]
24. Hollande, L.; Do Marcolino, I.; Balaguer, P.; Domenek, S.; Gross, R.A.; Allais, F. Preparation of Renewable Epoxy-Amine Resins with Tunable Thermo-Mechanical Properties, Wettability and Degradation Abilities from Lignocellulose- and Plant Oils-Derived Components. *Front. Chem.* **2019**, *7*, 159. [[CrossRef](#)] [[PubMed](#)]
25. Yu, M.; Fu, Q.; Zhang, T.; Chen, Y.; Tan, J.; Zhou, Y.; Zhu, X. Properties and curing kinetics of epoxy resin toughened by dimeric acid diglycidyl ester. *Thermochim. Acta.* **2021**, *699*, 178910. [[CrossRef](#)]
26. Hu, F.; Yadav, S.K.; La Scala, J.J.; Throckmorton, J.; Palmese, G.R. Epoxidized soybean oil modified using fatty acids as tougheners for thermosetting epoxy resins: Part 1. *J. Appl. Polym. Sci.* **2021**, *138*, e50570. [[CrossRef](#)]
27. Zhang, T.; Tan, J.; Han, X.; Fu, Q.; Chen, M.; Xu, Y.; Zhu, X. Novel epoxy-ended hyperbranched polyether derived from xylitol as sustainable tougheners for epoxy resin. *Polym. Test.* **2021**, *94*, 107053. [[CrossRef](#)]
28. Yadav, S.K.; Hu, F.; La Scala, J.J.; Palmese, G.R. Toughening Anhydride-Cured Epoxy Resins Using Fatty Alkyl-Anhydride-Grafted Epoxidized Soybean Oil. *ACS Omega* **2018**, *3*, 2641–2651. [[CrossRef](#)] [[PubMed](#)]
29. Mi, X.; Wei, F.; Zhong, L.; Zeng, L.; Zhang, J.; Xu, Z.; Zhang, D.; Miao, M. Epoxidation of agricultural byproduct konjac fly powder and utilization in toughening and strengthening epoxy resin. *Ind. Crops Prod.* **2020**, *146*, 112161. [[CrossRef](#)]
30. Cheung, Y.; Meenu, M.; Yu, X.; Xu, B. Phenolic acids and flavonoids profiles of commercial honey from different floral sources and geographic sources. *Int. J. Food Prop.* **2019**, *22*, 290–308. [[CrossRef](#)]
31. Ball, D.W. The Chemical Composition of Honey. *J. Chem. Educ.* **2007**, *84*, 1643–1646. [[CrossRef](#)]
32. Zakaria, M.R.; Abdul Kudus, M.H.; Md Akil, H.; Zamri, M.H. Improvement of Fracture Toughness in Epoxy Nanocomposites through Chemical Hybridization of Carbon Nanotubes and Alumina. *Materials* **2017**, *10*, 301. [[CrossRef](#)] [[PubMed](#)]
33. Demirci, M.; Tarakçıoğlu, N.; Avcı, A.; Akdemir, A.; Demirci, I. Fracture toughness (Mode I) characterization of SiO<sub>2</sub> nanoparticle filled basalt/epoxy filament wound composite ring with split-disk test method. *Compos. B Eng.* **2017**, *119*, 114–124. [[CrossRef](#)]
34. Rahmani, H.; Eslami-Farsani, R.; Ebrahimnezhad-Khaljiri, H. High velocity impact response of aluminum- carbon fibers-epoxy laminated composites toughened by nano silica and zirconia. *Fibers Polym.* **2020**, *21*, 170–178. [[CrossRef](#)]
35. Hao, S.; Yuan, J.; Cui, J.; Yuan, W.; Zhang, H.; Xuan, H. The rapid detection of acacia honey adulteration by alternating current impedance spectroscopy combined with <sup>1</sup>H NMR profile. *LWT* **2022**, *161*, 113377. [[CrossRef](#)]
36. Wang, H.Y.; Qian, H.; Yao, W.R. Melanoidins produced by the Maillard reaction: Structure and biological activity. *Food Chem.* **2011**, *128*, 573–584. [[CrossRef](#)]
37. Wegener, S.; Kaufmann, M.; Kroh, L.W. Influence of l-pyroglutamic acid on the color formation process of non-enzymatic browning reactions. *Food Chem.* **2017**, *232*, 450–454. [[CrossRef](#)]
38. Kozłowicz, K.; Różyło, R.; Gładyszewska, B.; Matwijczuk, A.; Gładyszewski, G.; Chocyk, D.; Samborska, K.; Piekut, J.; Smolewska, M. Identification of sugars and phenolic compounds in honey powders with the use of GC-MS, FTIR spectroscopy, and X-ray diffraction. *Sci Rep.* **2020**, *10*, 16269. [[CrossRef](#)]
39. Ciursa, P.; Pauliuc, D.; Dranca, F.; Ropciuc, S.; Oroian, M. Detection of honey adulterated with agave, corn, inverted sugar, maple and rice syrups using FTIR analysis. *Food Control.* **2021**, *130*, 108266. [[CrossRef](#)]
40. Bunaciu, A.A.; Aboul-Enein, H.Y. Honey Discrimination Using Fourier Transform-Infrared Spectroscopy. *Chemistry* **2022**, *4*, 848–854. [[CrossRef](#)]
41. Chowdhury, R.A.; Hosur, M.V.; Nuruddin, M.; Tcherbi-Narteh, A.; Kumar, A.; Boddu, V.; Jeelani, S. Self-healing epoxy composites: Preparation, characterization and healing performance. *J. Mater. Res. Technol.* **2015**, *4*, 33–43. [[CrossRef](#)]
42. Radovic, I.; Stajic, A.; Radisavljevic, A.; Veljkovic, F.; Cebela, M.; Mitic, V.; Radojevic, V. Solvent effects on structural changes in self-healing epoxy composites. *Mater. Chem. Phys.* **2020**, *256*, 123761. [[CrossRef](#)]
43. Oracz, J.; Zyzewicz, D. In vitro antioxidant activity and ftir characterization of high-molecular weight melanoidin fractions from different types of cocoa beans. *Antioxidants* **2019**, *8*, 560. [[CrossRef](#)] [[PubMed](#)]
44. ElFaham, M.M.; Mostafa, A.M.; Nasr, G.M. Unmanned aerial vehicle (UAV) manufacturing materials: Synthesis, spectroscopic characterization and dynamic mechanical analysis (DMA). *J. Mol. Struct.* **2020**, *1201*, 127211. [[CrossRef](#)]
45. Oikonomopoulos, I.; Perraki, T.; Tougiannidis, N. Ftir study of two different lignite lithotypes from neocene achlada lignite deposits in nw greece. *Bull. Geol. Soc. Greece.* **2017**, *43*, 2284. [[CrossRef](#)]
46. Anjos, O.; Campos, M.G.; Ruiz, P.C.; Antunes, P. Application of FTIR-ATR spectroscopy to the quantification of sugar in honey. *Food Chem.* **2014**, *169*, 218–223. [[CrossRef](#)]

47. Subari, N.; Mohamad Saleh, J.; Md Shakaff, A.Y.; Zakaria, A. A Hybrid Sensing Approach for Pure and Adulterated Honey Classification. *Sensors* **2012**, *12*, 14022–14040. [[CrossRef](#)] [[PubMed](#)]
48. Wu, D.Y.; Meure, S.; Solomon, D. Self-healing polymeric materials: A review of recent developments. *Prog. Polym. Sci.* **2008**, *33*, 479–522. [[CrossRef](#)]
49. Radovic, I.M.; Stojanovic, D.B.; Kojovic, A.; Petrovic, M.; Uskokovic, P.S.; Radojevic, V.J.; Aleksic, R.R. Healing efficiency of polystyrene electrospun nanofibers with Grubbs' catalyst in thermosetting composite. *J. Compos. Mater.* **2017**, *51*, 3003–3016. [[CrossRef](#)]
50. Icduygu, M.G.; Asilturk, M.; Yalcinkaya, M.A.; Hamidi, Y.K.; Altan, M.C. Three-Dimensional Nano-Morphology of Carbon Nanotube/Epoxy Filled Poly(methyl methacrylate) Microcapsules. *Materials* **2019**, *12*, 1387. [[CrossRef](#)]
51. Bellenger, V.; Fontaine, E.; Fleishmann, A.; Saporito, J.; Verdu, J. Thermogravimetric Study of Amine Cross-Linked Epoxies. *Polym. Degrad. Stab.* **1984**, *9*, 195–208. [[CrossRef](#)]
52. Wang, L.; Qiu, H.; Liang, C.; Song, P.; Han, Y.; Han, Y.; Gu, J.; Kong, J.; Pan, D.; Guo, Z. Electromagnetic Interference Shielding MWCNT-Fe<sub>3</sub>O<sub>4</sub>@Ag/Epoxy Nanocomposites with Satisfactory Thermal Conductivity and High Thermal Stability. *Carbon* **2019**, *141*, 506–514. [[CrossRef](#)]
53. Fei, X.; Wei, W.; Zhao, F.; Zhu, Y.; Luo, J.; Chen, M.; Liu, X. Efficient Toughening of Epoxy-Anhydride Thermosets with a Biobased Tannic Acid Derivative. *ACS Sustain. Chem. Eng.* **2017**, *5*, 596–603. [[CrossRef](#)]
54. Nooshkama, M.; Varidi, M.; Vermac, D.K. Functional and biological properties of Maillard conjugates and their potential application in medical and food: A review. *Food Res. Int.* **2020**, *131*, 109003. [[CrossRef](#)] [[PubMed](#)]
55. Chang, H.; Gilcher, E.B.; Huber, G.W.; Dumesic, J.A. Synthesis of performance-advantaged polyurethanes and polyesters from biomass-derived monomers by aldol-condensation of 5-hydroxymethyl furfural and hydrogenation. *Green Chem.* **2021**, *23*, 4355–4364. [[CrossRef](#)]
56. Engozogho Anris, S.P.; Bi Athomo, A.B.; Safou Tchiana, R.; Santiago-Medina, F.S.; Cabaret, T.; Pizzi, A.; Charrier, B. The condensed tannins of okoume (*Aucoumea klaineana* pierre): A molecular structure and thermal stability study. *Sci. Rep.* **2020**, *10*, 1773. [[CrossRef](#)] [[PubMed](#)]
57. Carbas, R.J.C.; Marques, E.A.S.; da Silva, L.F.M.; Lopes, A.M. Effect of Cure Temperature on the Glass Transition Temperature and Mechanical Properties of Epoxy Adhesives. *J. Adhes.* **2014**, *90*, 104–119. [[CrossRef](#)]
58. Courtois, A.; Hirsekorn, M.; Benavente, M.; Jaillon, A.; Marcin, L.; Ruiz, E.; Lévesque, M. Viscoelastic behavior of an epoxy resin during cure below the glass transition temperature: Characterization and modeling. *J. Compos. Mater.* **2018**, *53*, 155–171. [[CrossRef](#)]
59. Michel, M.; Ferrier, E. Effect of curing temperature conditions on glass transition temperature values of epoxy polymer used for wet lay-up applications. *Constr. Build. Mater.* **2020**, *231*, 117206. [[CrossRef](#)]
60. Yu, C.; Xu, Z.; Ma, X.; Zhang, J.; Chen, S.; Miao, M.; Chen, H.; Zhang, D. Hyperbranched polymers containing epoxy and imide structure. *Prog. Org. Coat.* **2021**, *151*, 106031. [[CrossRef](#)]

**Disclaimer/Publisher's Note:** The statements, opinions and data contained in all publications are solely those of the individual author(s) and contributor(s) and not of MDPI and/or the editor(s). MDPI and/or the editor(s) disclaim responsibility for any injury to people or property resulting from any ideas, methods, instructions or products referred to in the content.